

THE TIMING OF MINERALIZATION AT THE JACLYN ZONE GOLD DEPOSIT, CENTRAL NEWFOUNDLAND: CONSTRAINTS FROM $^{40}\text{Ar}/^{39}\text{Ar}$ STUDIES OF WHITE MICA ALTERATION ADJACENT TO AURIFEROUS QUARTZ VEINS

H.A. Sandeman
Mineral Deposits Section

ABSTRACT

The Jaclyn Zone gold deposit (the Golden Promise deposit), is located in the western Exploits Subzone of the central mobile belt of the Newfoundland Appalachian Orogen. The gold resource at the deposit is based upon a ~1-m-wide, north-east-trending and steeply southeast-dipping quartz-vein network termed the Jaclyn Main vein; this is only one of several such veins exposed in the deposit area. Vein textures are varied, including laminated- and comb-textured material and these are hosted by interlayered, mafic volcaniclastic arenite, siltstone and wacke of the Noel Paul's Brook Group of the Middle–Late Ordovician Victoria Lake supergroup. Regional metamorphic grade is low (sub-greenschist facies). The veins are developed in the uppermost strata of the supergroup, directly below the conformable transition to Sandbian (Caradocian) black shale. Native gold occurs as blebs in the comb-textured quartz and in the margins of laminated veins. Alteration in the footwall of the veins is dominated by illite+ankerite+Fe-chlorite+albite, whereas alteration in the immediate hanging wall is dominated by ankerite+albite+Fe-chlorite+illite+barian-potassium feldspar (adularia). The $^{40}\text{Ar}/^{39}\text{Ar}$ thermochronology on 2 samples from the immediate structural footwall of 2 major veins (Jaclyn Main and Christopher) indicate that the illite-dominated assemblage formed at ca. 428 Ma. The ankerite+Fe-chlorite+albite+illite+adularia-bearing assemblage in the hanging wall yielded a less robust age of ca. 400 Ma. Because the latter sample contains two distinct potassium-bearing phases, its younger age may be derived from a mixture of argon from sparse, ca. 428 Ma illite and from fine-grained and disseminated, younger (ca. 400–380 Ma?) adularia. Presently, the ca. 428 Ma age is interpreted to be the best estimate for the time of gold mineralization.

INTRODUCTION

The Jaclyn Zone gold deposit (Golden Promise deposit) occurs about 10 km southwest of the community of Badger in central Newfoundland (Figures 1 and 2). Discovered in 2002 by prospector William Mercer, the showing consisted of coarse-grained, comb-textured and stylolitic quartz boulders that were derived from underlying outcrops. A composite sample from ~10 of these boulders assayed ~30 g/t Au. The project was optioned by Rubicon Minerals Corporation and has since been explored under a number of joint-venture projects. Since 2002, the mineralization has been intensely explored (e.g., Copeland and Newport, 2004a, b, 2005; Pilgrim and Giroux, 2008; T. Tettelaar, personal communication, 2013). That work included, a regional airborne magnetic and electromagnetic survey, a regional soil-sampling program (6000 B-horizon samples), intensive prospecting and mapping, and 136 shallow (<314 m depth) NQ drill-holes totalling 22 529 m. A NI-43-101F1-compliant resource calculation on the Jaclyn Main zone (Pilgrim and

Giroux, 2008) outlined a total of 921 000 tonnes averaging 3.02 g Au/t (2.5 million contained grams of gold), with a cut-off grade of 1 g/t Au. In 2010, bulk sampling of 2174 metric tonnes to test the veracity of the diamond-drill hole-defined resource, yielded 8780.52 grams of gold (and 645.4 grams of Ag) for an average recovered ore gold grade of 5.59 g/t Au (Jet Metal Corporation, Press Release, April 20th, 2011; Sedar website). In addition, two detailed research-oriented investigations focussed on the nature and setting of the quartz veins (Newport, 2003; Sandeman *et al.*, 2010), and a third study examined the petrochemistry of the mafic dykes associated with the auriferous quartz veins (Sandeman and Copeland, 2010).

This contribution builds on the earlier work of Sandeman *et al.* (2010) and presents petrographic and mineral chemical information (confirmed by electron microprobe; H. Sandeman, unpublished data, 2013) on alteration immediately adjacent to the Jaclyn Main vein, constituting the resource calculation, as well as the Christopher vein,

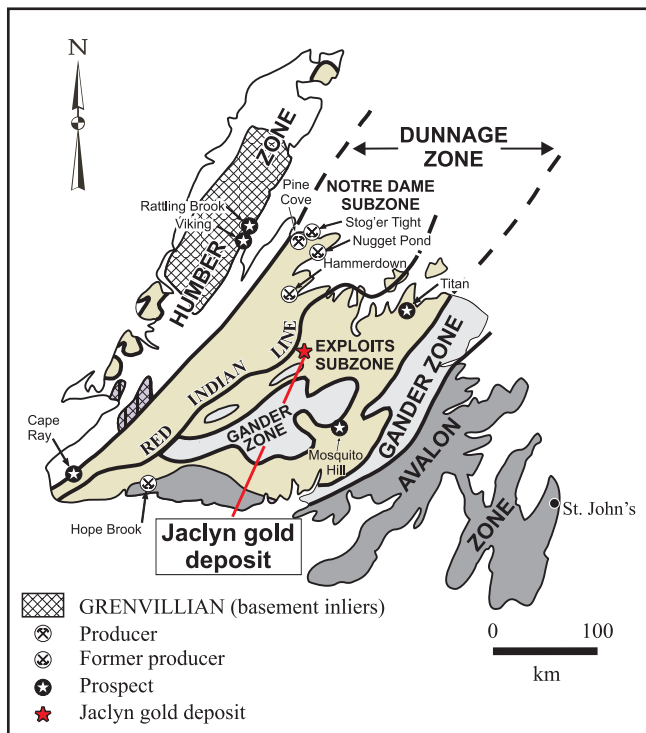


Figure 1. Location of the Jaclyn deposit in the western Exploits Subzone of the central Newfoundland Appalachians. Also shown are the locations of other gold deposits discussed in the text.

exposed 500 m to the southwest. Two $^{40}\text{Ar}/^{39}\text{Ar}$ ages are presented for illite from the immediate structural footwall of the two different veins and a third $^{40}\text{Ar}/^{39}\text{Ar}$ age is from the structural hanging wall of the Jaclyn Main vein. These data provide new insights into the mineral assemblages and age of the alteration associated with the auriferous quartz veins, which in turn provides constraints on the timing of gold mineralization.

REGIONAL SETTING

The Jaclyn gold deposit and several nearby auriferous quartz veins were collectively termed the Golden Promise Property (Mullen, 2003). The area lies within the Exploits Subzone of the Dunnage Zone of the Newfoundland Appalachians (Figure 1). The Dunnage Zone consists of accreted-arc, back-arc and intra-oceanic island terranes formed in the Iapetus Ocean during the Cambrian and Ordovician. A fundamental feature of the Dunnage Zone is the Red Indian Line, a major lithospheric-scale fault zone that juxtaposes rocks of the peri-Gondwanan Exploits Subzone, to the southeast, against peri-Laurentian oceanic rocks of the Notre Dame Subzone to the northwest (Williams *et al.*, 1988; Williams, 1995). The trace of the Red Indian Line is located approximately 8 km to the west of the Jaclyn gold deposit (Figure 2).

The Exploits Subzone is underlain by a structurally imbricated series of lithologically diverse, arc-back-arc volcano-sedimentary assemblages that include the Tulks Hill, Long Lake and Tally Pond belts as well as the sedimentary-dominated Harpoon Brook belt (Evans and Kean, 2002; Rogers and van Staal, 2002). These are collectively known as the Victoria Lake supergroup (VLS; Evans and Kean, 2002; Rogers and van Staal, 2002). The immediate study area is underlain by marine volcaniclastic sedimentary rocks initially termed the Harpoon Brook belt (Evans and Kean, 2002) but have recently been assigned to the Noel Paul's Brook Group (Rogers *et al.*, 2005). The oldest rocks of the Noel Paul's Brook Group are green-grey shale and mudstone, volcaniclastic sandstone and wacke collectively considered to represent turbidites (Kean and Jayasinge, 1982). These form a megascopic, north- and west-facing sequence that fines upward away from the major volcanic centres of the Tulks Hill, Long Lake and Tally Pond belts. These turbiditic sedimentary rocks were assigned to the Stanley Waters formation (Rogers *et al.*, 2005).

The Stanley Waters formation is described as being conformably overlain by pyritic and graphitic black shale that, on the basis of graptolite fauna (e.g., Williams and O'Brien, 1991), are Sandbian (Caradocian). Contacts between the Sandbian shale and the Stanley Waters formation are typically sheared and structurally complex, but have locally been reported as conformable (e.g., Kean and Jayasinge, 1982; Williams, 1991). The Sandbian graphitic shales are assigned to the Lawrence Harbour Formation, the uppermost strata of the Victoria Lake supergroup (Rogers *et al.*, 2005). The Lawrence Harbour Formation is inferred to be conformably overlain by the continentally derived, fore-arc overlap-sequence rocks of the Ordovician–Silurian Badger Group (Williams, 1995; van Staal, 2007), however, most of the exposed contacts are structurally complex and highly strained and primary relationships are uncertain (cf., Williams, 1991 *versus* McNeill, 2005, *in* Copeland and Newport, 2005). Rocks of the Badger Group comprise grey-blue sandstone with less common, grey-black shale interbeds and rip-ups that are overlain by polymictic conglomerate. These rocks are considered to be dominantly derived from the topographically uplifted rocks of the Notre Dame Subzone to the west (Waldron *et al.*, 2012) and deposited in a restricted fore-arc oceanic basin immediately prior to final closure of Iapetus Ocean in the Silurian Salinic orogeny (Dunning *et al.*, 1990; van Staal, 2007; van Staal *et al.*, *in press*). All units are cut by an array of northeast- to southeast-trending fine-grained diabase dykes termed the Exploits dykes (McNeill, 2005 *in* Copeland and Newport, 2005; Sandeman and Copeland, 2010).

The rocks of the region exhibit four generations of structures. The oldest are cryptic, early thrust faults having a strong, locally developed cleavage. Second-generation

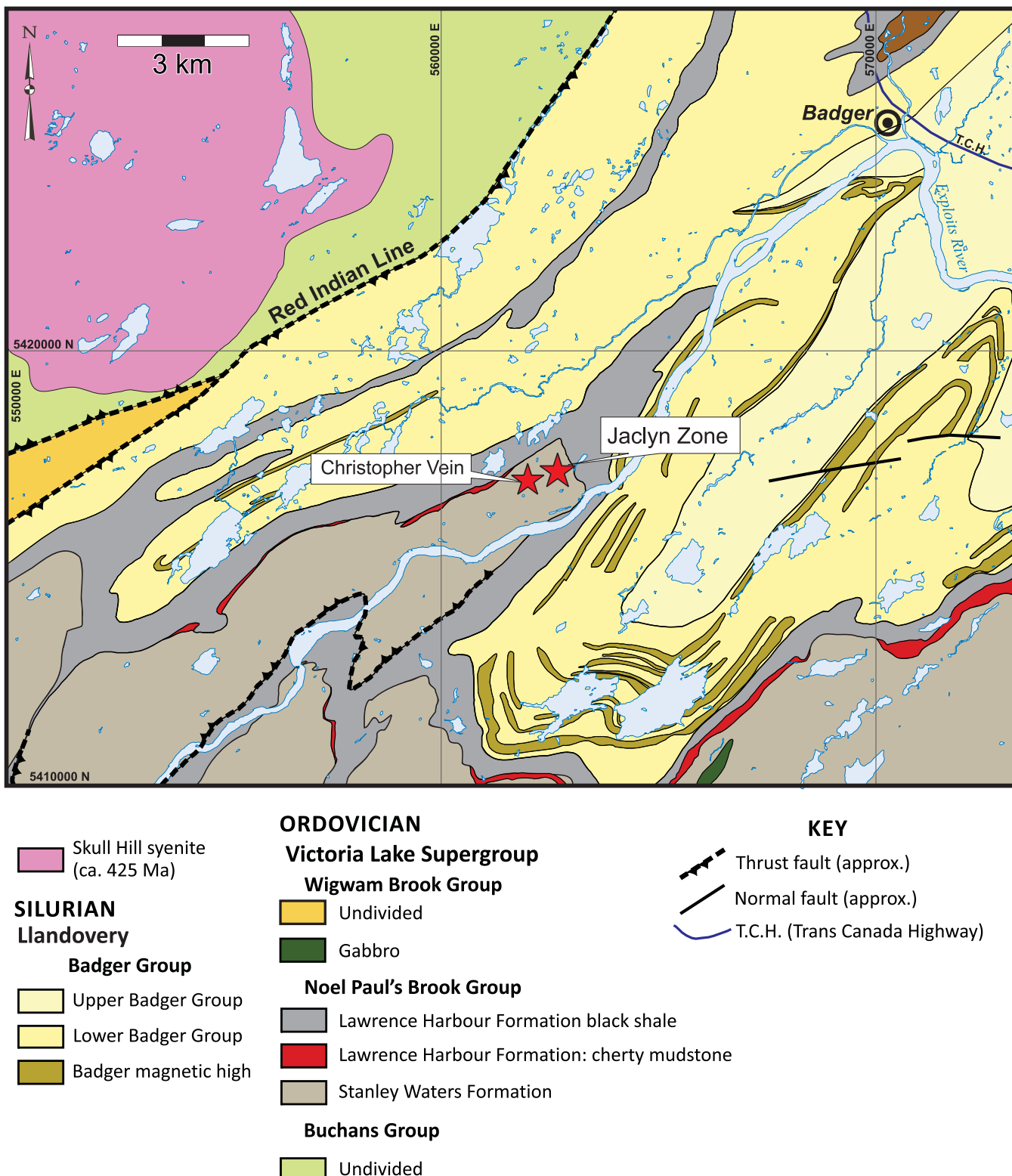


Figure 2. Simplified geological map of the region (adapted from McNeill, 2005 in Copeland and Newport, 2005, and Rogers et al., 2005) showing the location of the Jaclyn veins at the inferred top of the Stanley Waters formation of the Victoria Lake supergroup. Units of the Badger Group are largely defined using detailed airborne magnetic and resistivity data.

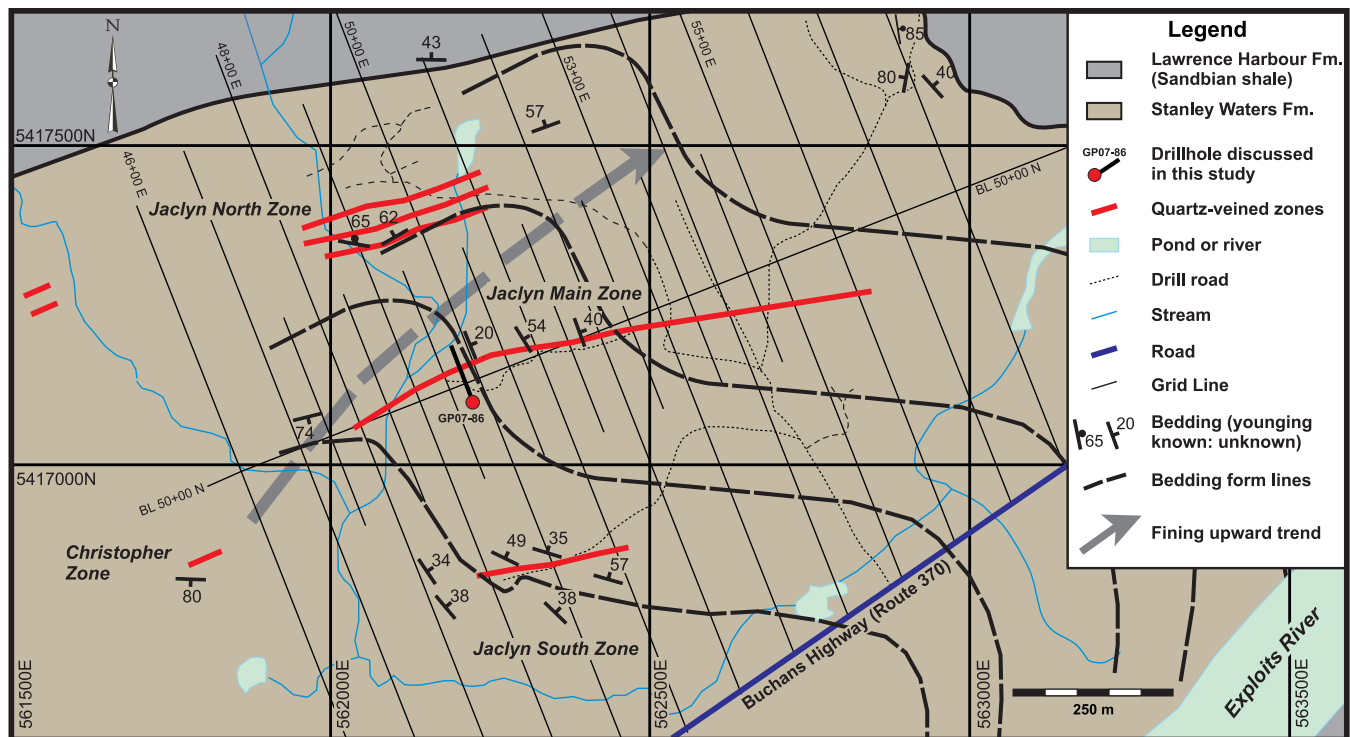


Figure 3. Map of the Jaclyn Zone area showing the location of the vein systems relative to drainage and access trails. Also shown are the locations of the drillhole GP07-86 and the Christopher zone. The few bedding measurements from trenches and the inferred trace of bedding are indicated. The large shaded arrow denotes the megascopic fining upward trend in the sedimentary rocks toward the contact between the Stanley Waters and Lawrence Harbour formations. Geological contact is inferred from detailed airborne magnetic and resistivity data and drillhole intercepts.

structures fold the Badger Group and Victoria Lake supergroup into km-wavelength-scale, upright to inclined, doubly plunging (primarily to the northeast; McNeill, 2005 *in Copeland and Newport, 2005*) folds. These are southeast-verging, tight, chevron-style antiform–synform pairs that commonly exhibit broken limbs that are cut by, and likely locally transposed into, small-scale, limb-parallel reverse faults. These dominate the regional map pattern (Figure 2). The third-generation structures are less conspicuous, large wavelength (~6 km), open folds that variably plunge to the southeast and have steeply dipping southeast-trending axial planes. Both regional-scale fold sets exhibit uncommon, outcrop-scale, macroscopic equivalents (McNeill, 2005 *in Copeland and Newport, 2005*). The area is transected by several northwest- and northeast-trending late brittle faults that crosscut older structures.

JACLYN DEPOSIT GEOLOGY AND MINERALIZATION

The gold resource estimate at the Jaclyn deposit is based upon the most extensive of four auriferous quartz veins recognized in the area. From south to north these comprise: the Jaclyn South, the Christopher, the Jaclyn Main

and, the Jaclyn North veins (Figure 3); the resource is contained within the Jaclyn Main vein. Bedrock in the area was only encountered *via* trenching or through diamond drilling, although boulder-train analysis greatly assisted in delimiting the extent and location of the veins.

These vein systems are collectively hosted by the uppermost stratigraphic levels of the Stanley Waters formation, consisting of wacke, sandstone and siltstone that are dominated by plagioclase-rich, intermediate to mafic volcanic and fine-grained pelagic sedimentary detritus. The beds are upright and typically fine upward to the northeast. These rocks form the core of a 2- to 3-km wavelength, tight, moderately northeast-plunging and southeast-verging F_1 anticline that folds the Stanley Waters formation, black, pyritic Sandbian shale of the Lawrence Harbour Formation and the turbiditic sedimentary rocks of the Badger Group (MacNeill, 2005 *in Copeland and Newport, 2005*; Rogers *et al.*, 2005).

CHRISTOPHER ZONE

The Christopher vein is located approximately 500 m to the southwest of the Jaclyn zones (Figure 3). The vein trends

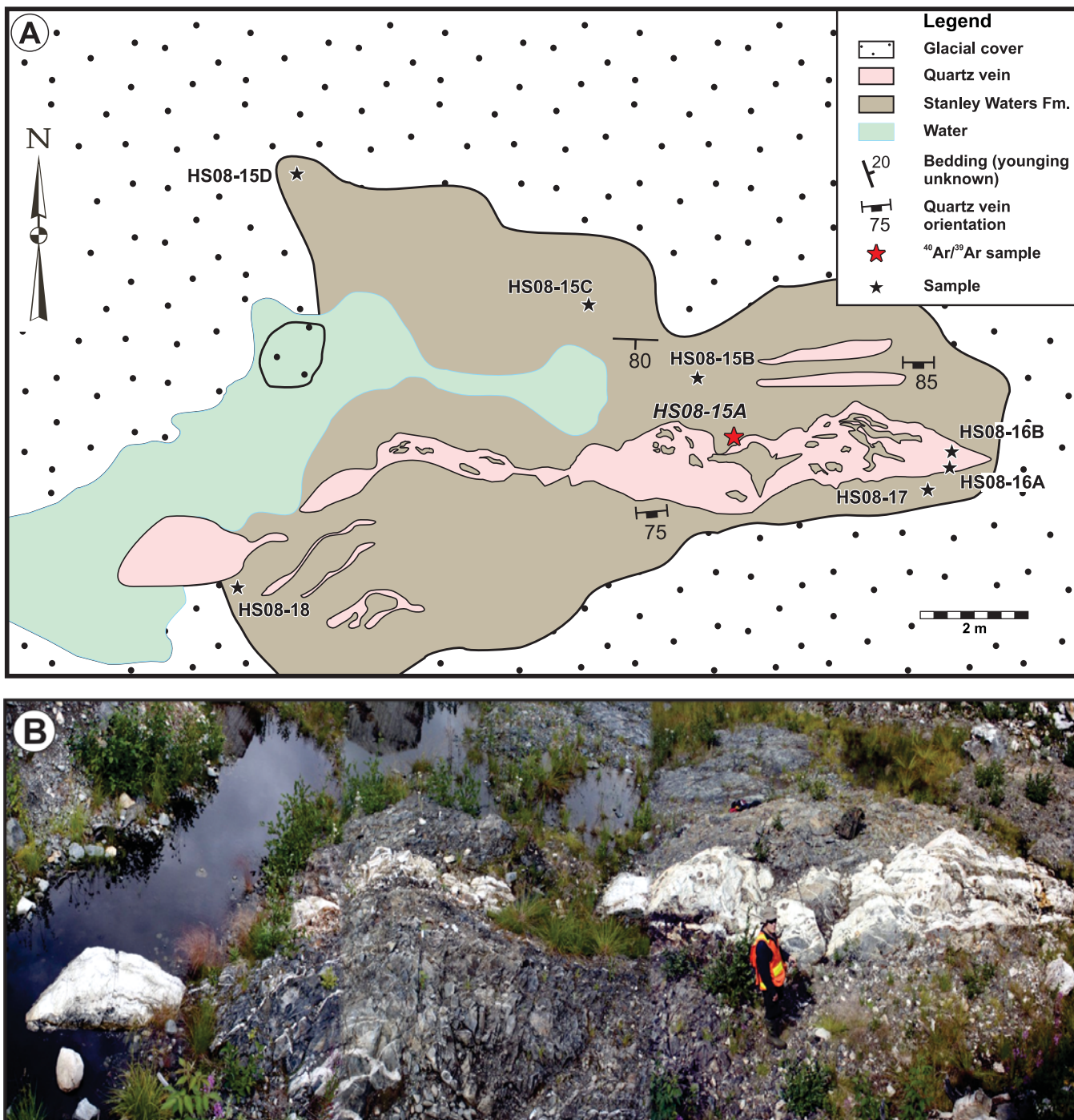


Figure 4. A) Sketch map of the Christopher zone trench showing the orientation, width and inclusion-rich character of the auriferous quartz vein (up to 3.6 g/t Au) and the location of $^{40}\text{Ar}/^{39}\text{Ar}$ thermochronological sample HS08-15A; B) Photograph illustrating the pinch and swell character of the Christopher vein.

085°/75°S and ranges in width from <1 to 3 m. It has stylolitic margins, locally with a coarse-grained, comb-textured interior and contains abundant country-rock inclusions (Figure 4). Visible gold has been found in outcrop, but the best outcrop assay returned a value of only 1.96 g/t Au with strongly elevated arsenic. Limited drilling (2 holes) returned

a maximum of 0.3 g/t Au over 0.7 m, accompanied by anomalous arsenic (Copeland and Newport, 2004a, b, 2005) that was interpreted to indicate that the grades are generally lower than at the Jaclyn Main zone. At surface, the wall-rocks to the Christopher vein are dominated by epiclastic(?) sandstone and wackes containing minor siltstone and mud-

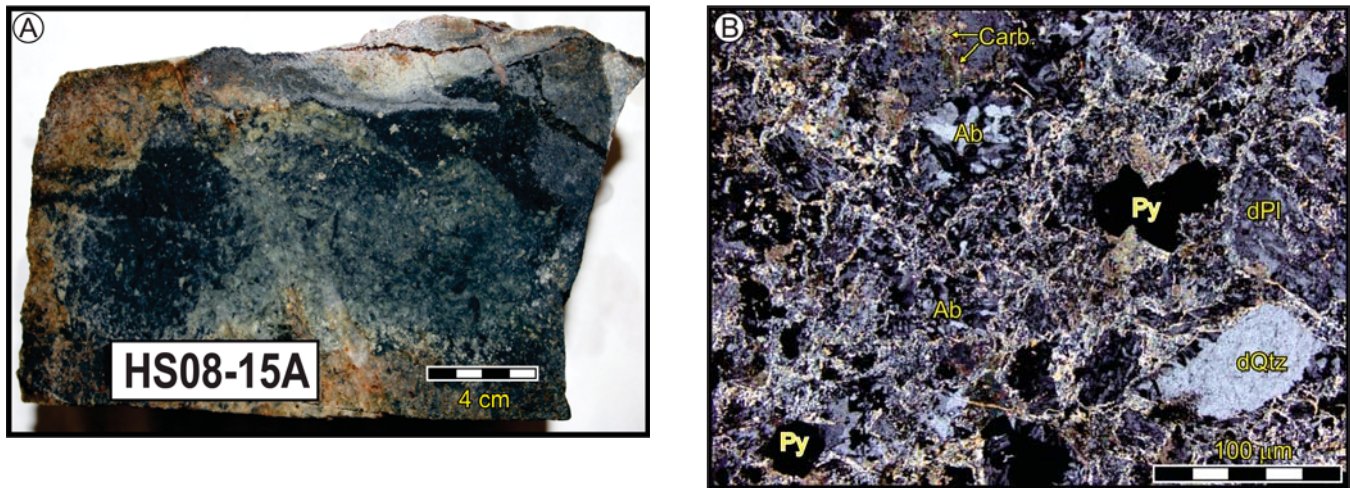


Plate 1. A) Slab photograph of intensely illite+albite+ankerite+chlorite+pyrite-altered lithic arenite (sample HS08-15A) from the immediate structural footwall of the Christopher vein; B) Photomicrograph of sample HS08-15A showing the extensive replacement of the matrix of the arenite by intimately intergrown illite (high birefringent laths), ankerite (Carb), albite (Ab) and pyrite (Py). Note the altered detrital plagioclase (dPl) and embayed quartz (dQtz).

stone intervals. Alteration of the coarse-grained clastic sedimentary rocks in the structural footwall of the vein is subtle, but comprises bleaching of the rocks' matrix accompanied by an increase in sulphides (typically pyrite) along with illite, calcite, ankerite, chlorite and local hematite. Petrographic study confirms that in the structural footwall, the matrix is extensively altered, whereas spotting is locally developed in thin mudstone intervals. The matrix of the medium-grained sandstone in the structural hanging wall of the vein is extensively altered to an ankerite+albite+hematite-bearing assemblage.

The matrix of the plagioclase-rich wacke (sample HS08-15A) from the immediate footwall of Christopher vein is intensely altered (Plate 1). The alteration has resulted in extensive replacement of the wacke matrix by intimately intergrown illite+albite+ankerite+calcite+chlorite. This sample was dated using the $^{40}\text{Ar}/^{39}\text{Ar}$ method.

JACLYN MAIN ZONE

The Jaclyn Main zone contains several major, east-northeast-trending (~080/80°) quartz veins that contain minor sulphides and visible gold. The widest and most significant is the Jaclyn Main vein (Figure 3). Wallrocks are dominated by medium- to coarse-grained feldspathic sandstone and mudstone-clast-bearing feldspathic wacke, and metre-scale intercalated beds of varicoloured siltstone and mudstone. Bleaching and spotting of the fine-grained host rocks is common, particularly near the veins. The quartz veins have laminated chlorite-rich stylolitic margins and coarse-grained, comb-textured interiors (Mullen, 2003; Sandeman *et al.*, 2010). The stylolitic margins of the veins contain foliated, chlorite-altered siltstone septae or bands

that locally terminate quartz and quartz carbonate veins in the wallrocks. The stylolitic vein margins also locally contain soft, gouge-like material or breccia-like zones of illite+ankerite+calcite+chlorite+albite-altered, fine-grained siltstone fragments. Within 2 m of the Jaclyn Main vein, host siltstones typically exhibit strong bleaching, which occurs in irregular patches and anastomosing channel-like zones (Sandeman *et al.*, 2010). In siltstones, up to 15 m from the vein, a spotted, bleached texture is very common but is not definitively genetically related to the Au-bearing quartz veins (Tarnocai, 2004; Sandeman *et al.*, 2010). The veins and host rocks are locally cut by at least two distinct suites of mafic dykes, one set of which is contemporaneous with the auriferous quartz veins (Sandeman and Copeland, 2010).

In drillhole GP07-86, a 60-cm-wide, auriferous quartz vein occurs at a depth of 94.85–95.45 m and contains 2.84 g/t Au over that 60 cm interval (Plate 2A). Intense alteration and bleaching, forming channel-like conduits (Plate 2B) and spotted zones occur in the immediate hanging wall of the vein (sample GP07-86_94.7: Plate 2C). These bleached zones and spots in the structural hanging wall are characterized by intergrown ankerite, albite, calcite, illite, chlorite and potassium feldspar (adularia?). The intensely bleached portion of this sample was dated using the $^{40}\text{Ar}/^{39}\text{Ar}$ method. Immediately below the vein is a 5-cm-wide zone of breccia consisting of angular altered fragments of siltstone enclosed in an anastomosing network of similarly altered siltstone flour (sample GP07-86_95.45: see Plate 2B). The breccia fragments and their matrix contain intergrown illite, ankerite, albite, calcite and chlorite with abundant anhedral grains of galena, sphalerite and intergrown pyrite and chalcopyrite. This altered breccia material was also dated using $^{40}\text{Ar}/^{39}\text{Ar}$ thermochronology.

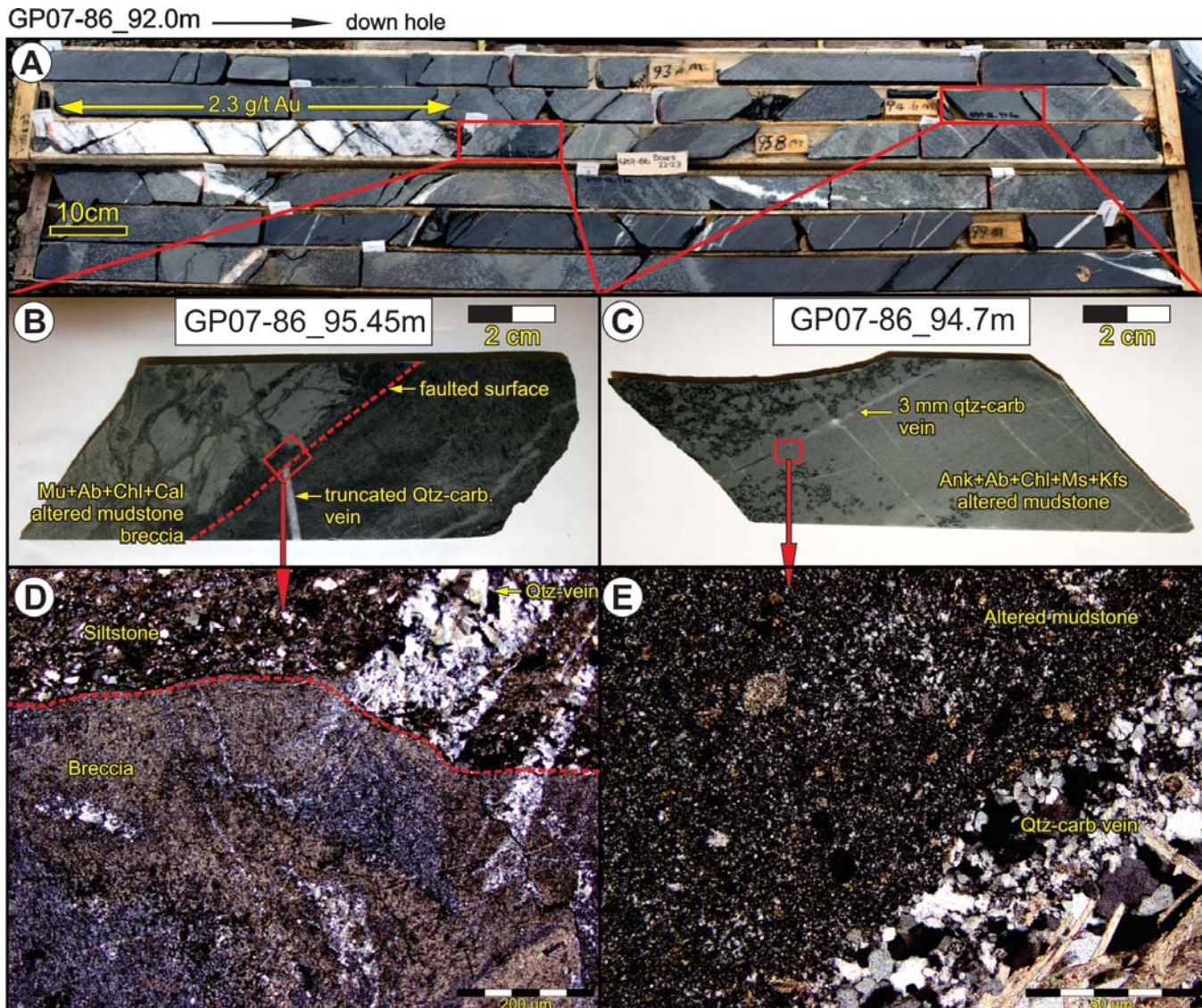


Plate 2. A) Photograph of core boxes 22 and 23 from diamond-drill hole GP-07-86 showing the locations of the two specimens (GP07-86_95.45 m and GP07-86_94.7 m) in relationship to the 60-cm-wide, Jaclyn Main vein intercept. These samples were investigated using petrographic methods, Visual and Infrared spectrometric analysis (VIRS: Sandeman *et al.*, 2010), electron probe microanalysis (H. Sandeman, unpublished data, 2013) and $^{40}\text{Ar}/^{39}\text{Ar}$ thermochronology; B) Slab photograph of sample GP07-86_95.45 m; C) Slab photograph of sample GP07-86_94.7 m; D) Photomicrograph of GP07-86_95.45 m; E) Photomicrograph of GP07-86_94.7 m.

At Jaclyn North (Figure 3), west-southwest-trending, moderately northwest-dipping, fine- to very-fine-grained, green to black cherty mudstone and siltstone predominate in trench exposures. In drillholes, these pass gradationally downward into grey, mudstone-clast-bearing wacke and plagioclase-rich and feldspathic air fall tuff (Copeland and Newport, 2004a, b, 2005; Sandeman *et al.*, 2010; T. Tette-laar, personal communication, 2013). The proportion of coarse-grained sedimentary rocks increases downhole, and local graded beds indicate younging to the northwest and

east (Figure 3). Three irregular, stylolitic and inclusion-rich, bedding-parallel quartz veins and veined zones up to 9.6 m wide have been intersected in drillcore at Jaclyn North.

$^{40}\text{Ar}/^{39}\text{Ar}$ AGE DATA

The $^{40}\text{Ar}/^{39}\text{Ar}$ age determinations were obtained at the Queen's University $^{40}\text{Ar}/^{39}\text{Ar}$ Thermochronology Laboratory using the methods outlined by Minnett *et al.* (2012). The gas steps used in the calculation of the plateau ages are marked by bold type in Table 1 and by shaded boxes in Figure 5. All

Table 1. The $^{40}\text{Ar}/^{39}\text{Ar}$ thermochronological data for hydrothermal illite grain concentrates from three samples of altered host rocks immediately adjacent to the Jaclyn Main and Christopher veins

Lab #: D-672
 Sample: HS08-15A illite
 J Value: 0.016899 ± 0.000034
 Integrated age = 429.2 ± 1.1 Ma

Age = 427.8 ± 1.4 Ma
 (2 σ , including J-error of 0.25%)
 MSWD = 0.88, probability = 0.49
 49.9% of the 39Ar, steps 9 through 14

Power	$^{36}\text{Ar}/^{40}\text{Ar}$	+/-	$^{39}\text{Ar}/^{40}\text{Ar}$	+/-	r	K/Ca	% $^{40}\text{Ar}_{\text{Atm}}$	$^{40}\text{Ar}^{*}/^{39}\text{K}$	+/-	% ^{39}Ar	Age	+/-
1.8	0.003001	0.000047	0.01058	0.000091	0.011	5.24	88.64	10.71	1.36	0.48	300.1	35.2
2.0	0.001722	0.00005	0.029796	0.000249	0.007	3.18	50.84	16.48	0.53	0.56	443.3	12.5
2.3	0.001065	0.000028	0.040948	0.00021	0.008	0.83	31.43	16.74	0.22	2.53	449.3	5.3
2.5	0.000303	0.000017	0.056148	0.00025	0.003	0.57	8.93	16.22	0.12	3.62	437.0	2.8
2.7	0.000203	0.000014	0.058129	0.00027	0.003	0.93	5.98	16.17	0.10	8.73	435.9	2.5
2.8	0.000074	0.000015	0.061275	0.000286	0.001	1.34	2.18	15.96	0.11	7.98	430.9	2.6
2.9	0.000042	0.000012	0.061833	0.000269	0.001	1.83	1.24	15.97	0.09	5.26	431.1	2.2
3.0	0.000056	0.000011	0.061575	0.000257	0.001	3.41	1.66	15.97	0.09	12.38	431.0	2.1
3.1	0.000046	0.000012	0.062147	0.000272	0.001	12.05	1.35	15.87	0.09	8.90	428.7	2.2
3.2	0.000064	0.000011	0.061825	0.000262	0.001	17.24	1.89	15.87	0.09	9.78	428.6	2.1
3.3	0.00006	0.000012	0.061902	0.000277	0.001	20.41	1.77	15.87	0.09	8.19	428.6	2.3
3.4	0.000066	0.000016	0.061967	0.000251	0.001	24.39	1.96	15.82	0.10	6.55	427.5	2.5
3.5	0.000065	0.000015	0.062195	0.000265	0.001	27.78	1.93	15.77	0.10	4.81	426.2	2.4
3.7	0.000077	0.000012	0.061885	0.000276	0.001	23.26	2.26	15.79	0.09	11.61	426.8	2.2
3.9	0.000083	0.000017	0.062025	0.00028	0.001	17.24	2.44	15.73	0.11	3.96	425.2	2.6
4.2	0.000162	0.000022	0.060992	0.000314	0.002	8.93	4.78	15.61	0.13	1.95	422.4	3.2
6.0	0.000585	0.000024	0.053651	0.000271	0.007	1.91	17.23	15.42	0.15	2.69	417.8	3.7

Lab #: D-668
 Sample: GP07-86_95.45 m illite
 J Value: 0.016901 ± 0.000036
 Integrated age = 429.8 ± 1.2 Ma

Age = 427.9 ± 1.7 Ma
 (2 σ , including J-error of 0.25%)
 MSWD = 0.36, probability = 0.78
 39.1% of the 39Ar, steps 9 through 12

Power	$^{36}\text{Ar}/^{40}\text{Ar}$	+/-	$^{39}\text{Ar}/^{40}\text{Ar}$	+/-	r	K/Ca	% $^{40}\text{Ar}_{\text{Atm}}$	$^{40}\text{Ar}^{*}/^{39}\text{K}$	+/-	% ^{39}Ar	Age	+/-
1.6	0.003361	0.000135	0.007627	0.000286	0.003	2.54	99.30	0.89	5.26	0.06	26.9	158.1
2.0	0.001091	0.000034	0.051153	0.000255	0.012	2.39	32.18	13.25	0.21	1.51	364.5	5.3
2.3	0.000224	0.000019	0.058844	0.000358	0.005	0.61	6.62	15.87	0.14	4.23	428.6	3.3
2.5	0.000080	0.000015	0.060192	0.000341	0.002	0.47	2.36	16.22	0.12	4.47	437.1	2.9
2.7	0.000057	0.000015	0.060719	0.000403	0.001	0.64	1.67	16.19	0.13	8.49	436.4	3.2
2.9	0.000034	0.000015	0.061549	0.000387	0.001	1.37	1.01	16.08	0.12	9.57	433.8	3.0
3.1	0.000026	0.000012	0.061898	0.000272	0.000	8.77	0.75	16.03	0.09	10.76	432.6	2.2
3.3	0.000026	0.000014	0.062137	0.000290	0.001	20.41	0.76	15.97	0.10	15.61	431.1	2.4
3.5	0.000026	0.000012	0.062476	0.000347	0.001	37.04	0.78	15.88	0.11	15.40	429.0	2.5
3.7	0.000029	0.000018	0.062686	0.000291	0.000	31.25	0.87	15.81	0.11	12.79	427.3	2.7
3.9	0.000033	0.000013	0.062579	0.000329	0.001	26.32	0.96	15.83	0.10	6.76	427.6	2.5
4.2	0.000059	0.000015	0.062096	0.000275	0.000	16.95	1.74	15.82	0.10	4.14	427.6	2.4
4.7	0.000125	0.000014	0.060264	0.000255	0.001	6.99	3.68	15.98	0.10	3.21	431.4	2.4
6.0	0.000282	0.000018	0.056947	0.000273	0.003	2.27	8.31	16.10	0.12	3.01	434.2	2.9

Lab #: D-685
 Sample: GP07-86_94.7 m illite+adularia
 J Value: 0.016904 ± 0.000036
 Integrated age = 400 ± 8 Ma

Age = 400 ± 7 Ma
 (2 σ , including J-error of 0.25%)
 MSWD = 1.8, probability = 0.091
 74.1% of the 39Ar, steps 3 through 10

Power	$^{36}\text{Ar}/^{40}\text{Ar}$	+/-	$^{39}\text{Ar}/^{40}\text{Ar}$	+/-	r	K/Ca	% $^{40}\text{Ar}_{\text{Atm}}$	$^{40}\text{Ar}^{*}/^{39}\text{K}$	+/-	% ^{39}Ar	Age	+/-
1.8	0.002904	0.000227	0.011087	0.000524	0.004	0.00	85.70	12.87	6.1	2.10	355.2	152.8
2.1	0.000669	0.000092	0.057138	0.000686	0.004	2.60	19.70	14.05	0.51	21.67	384.4	12.5
2.3	0.000191	0.000106	0.066216	0.000824	0.000	2.54	5.62	14.25	0.51	16.18	389.4	12.4
2.5	0.000092	0.000122	0.064244	0.001029	0.000	5.68	2.70	15.14	0.61	14.29	411.2	14.9
2.7	0.000155	0.000155	0.062677	0.001000	0.000	10.00	4.57	15.22	0.77	11.34	413.2	18.7
3.0	0.000270	0.000147	0.063026	0.001019	0.003	5.68	7.94	14.6	0.73	12.20	398.1	17.9
3.3	0.000573	0.000304	0.061958	0.001235	0.002	2.28	16.85	13.42	1.48	6.17	368.7	36.7
3.6	0.000643	0.000291	0.057377	0.001274	0.002	1.19	18.88	14.13	1.54	5.78	386.5	37.8
4.0	0.000721	0.000224	0.052487	0.001117	0.003	1.26	21.17	15.01	1.31	5.82	408	31.8
4.5	0.001127	0.000442	0.040195	0.001450	0.004	0.59	33.14	16.62	3.33	2.33	446.8	79.2
6.0	0.001469	0.000347	0.023990	0.001152	0.003	0.75	43.21	23.66	4.47	2.13	606.9	97.4

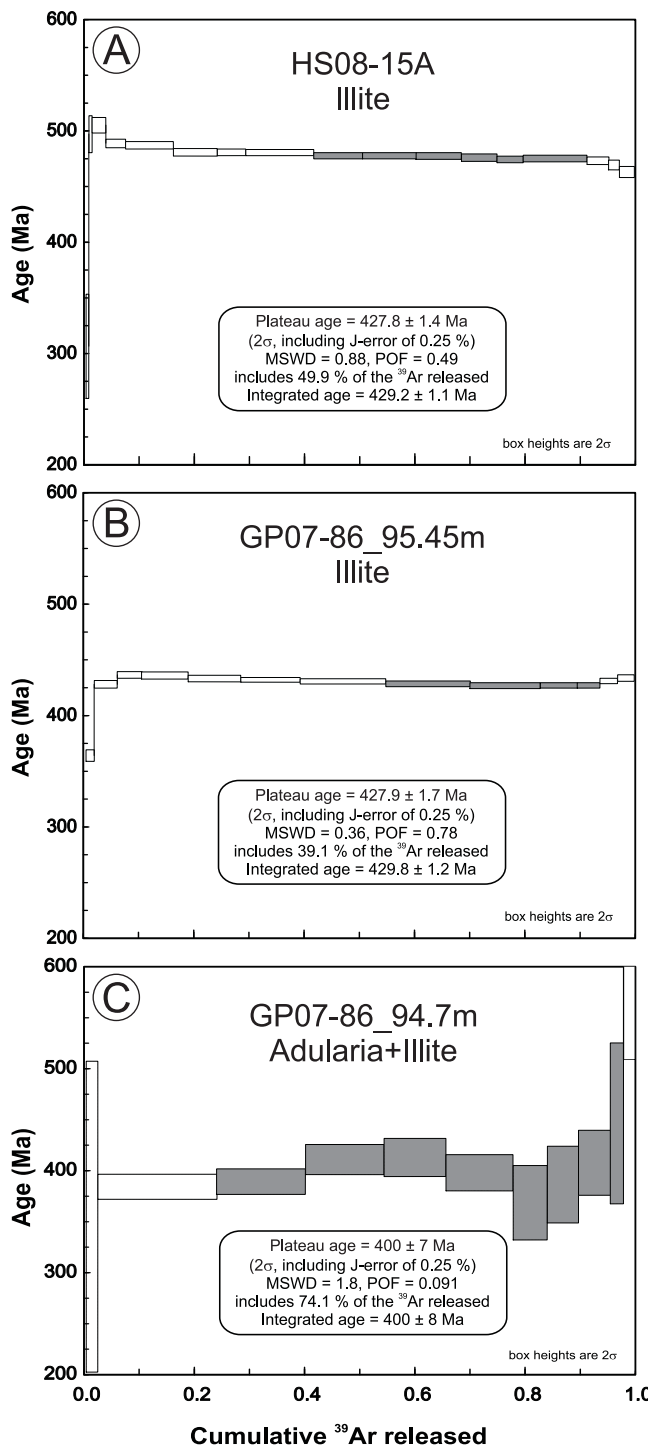


Figure 5. The $^{40}\text{Ar}/^{39}\text{Ar}$ age spectra for white mica grain separates from three specimens of altered wall rock adjacent to veins from the Jaclyn deposit area. A) HS08-15A; structural footwall to the Christopher vein; B) GP07-86_95.45; structural footwall to the Jaclyn Main vein; C) GP07-86_94.7; structural hanging wall to the Jaclyn Main vein.

age calculations used the $^{40}\text{Ar}/^{39}\text{Ar}$ age spectrum module of Ludwig (2003). $^{40}\text{Ar}/^{39}\text{Ar}$ plateau ages are typically defined by at least 3 contiguous gas release steps (consisting of $>60\%$ of released ^{39}Ar), with $^{40}\text{Ar}/^{39}\text{Ar}$ ages overlapping within 2σ error (McDougall and Harrison, 1988 and references therein; Snee *et al.*, 1988; Singer and Pringle, 1996). A plateau must also be defined by $^{40}\text{Ar}/^{39}\text{Ar}$ steps with reasonably low excess scatter (MSWD <2.2). These criteria were not fully satisfied by two of the three gas-release spectra for the samples under investigation. These two analyses yielded quasi-plateaux that do not fully satisfy the above criteria (Table 1; Figure 5), however, their internal consistency, high K/Ca ratios for concurrent steps and, small volumes of contained atmospheric argon indicate that these quasi-plateaux are likely representative of the cooling ages of the dominant potassium-bearing phases in the grain separates. The approximate argon closure temperatures for muscovite ($\sim 300^\circ\text{C}$) and potassium feldspar ($\sim 150^\circ\text{C}$) aid the interpretation of the cooling history of the host rocks (McDougall and Harrison, 1988; Reynolds, 1992). Preliminary fluid inclusion analysis (H. Sandeman, unpublished data, 2013) indicates that the fluids associated with deposition of the quartz veins were low salinity (4–10 wt% equivalent NaCl) and on the order of $\sim 275^\circ\text{C}$. This is below the closure temperature for muscovite, but above that for low-temperature potassium feldspar (adularia). The illite grain concentrate ages presented below are therefore inferred to represent the time of argon closure in the micas. Age uncertainties for all results are quoted at the 2σ uncertainty level.

The $^{40}\text{Ar}/^{39}\text{Ar}$ laser step-heating ages were determined for grain separates (175–250 μm), dominated by very fine-grained, randomly oriented white mica, extracted from three samples of altered and mineralized siltstone and sandstone adjacent to the Jaclyn Main and Christopher veins. The white mica is typically $\leq 50 \mu\text{m}$ long, too small to ensure pure mineral separates. These grain separates, therefore, represent white mica concentrates and contain other fine-grained mineral phases. HS08-15A is an altered sandstone obtained from the immediate structural footwall of the Christopher vein (*see above*). Sample GP07-86_95.45m is an altered mudstone from the immediate structural footwall, and GP07-86_94.7m is an altered mudstone from the hanging wall of the Jaclyn Main vein. Both samples were described in the preceding section.

An illite concentrate from sample HS08-15A (Christopher vein) yields a well-defined argon release spectrum characterized by an abrupt rise in the ages of the lowest temperature gas release steps, and the remainder of the spectrum consisting of a relatively flat segment having consistently younger ages for each successively higher temperature gas fraction (Figure 5A). Six consecutive steps (steps 9–14) overlap, within error, comprising 49.9% of the total ^{39}Ar released, and yield a quasi-plateau age of 427.8 ± 1.4 Ma

(MSWD=0.88: POP= 0.49). The quasi-plateau age overlaps, within error, with the integrated age of 429.2 ± 1.1 Ma. The age of 427.8 ± 1.4 Ma is therefore interpreted to represent the time of formation of the illite alteration and hence the age of the hydrothermal event responsible for deposition of the mica.

Illite from GP07-86_95.45m, in the immediate structural footwall of the Jaclyn Main vein, yields a well-defined argon release spectrum characterized by a rapid rise in the ages of the lowest temperature gas release steps, to the remainder of the spectrum consisting of a relatively flat segment with progressively younger ages for each successively higher temperature gas fraction (Figure 5B). The final two gas fractions yield slightly older ages. Four of the high temperature steps (fractions 9–12 of 14), represent 39.1% of the total ^{39}Ar released, and yield a quasi-plateau age of 427.9 ± 1.7 Ma (MSWD=0.36: POP= 0.78). Although this result is a quasi-plateau age, it is identical, within error, to the integrated age of 429.8 ± 1.2 Ma. Moreover, this age is also identical, within error, to that of HS08-15A, and is therefore also interpreted to represent the age of the hydrothermal event responsible for deposition of the mica.

An illite grain separate from the immediate structural hanging wall of the Jaclyn Main vein (GP07-86_94.7m) yielded a significantly different, mildly humped, argon release spectrum (Figure 5C). The ages of the gas fractions abruptly rise to a rough, humped plateau at *ca.* 400 Ma, and then rise again to significantly older ages in the high temperature gas fractions. Each individual gas fraction is characterized by large errors, relative to those of the other two spectra, and the plateau age has a corresponding large error. Gas release steps 3 through 10 yield a plateau age of 400 ± 7 Ma, representing 74.1% of the ^{39}Ar released (MSWD = 1.8: POF = 0.091). This overlaps, within error, with the total gas integrated age of 400 ± 8 Ma, but is significantly younger than the age determination for the illite alteration in the vein footwall, only 0.75 m downhole. It is important to note that the sample from the hanging wall (GP07-86_94.7m) yielded much lower K/Ca ratios and correspondingly higher atmospheric argon for each individual gas step (Table 1). Furthermore, this sample contains two distinct potassium-bearing minerals (illite and adularia) but these are far less abundant than in samples obtained from the footwall alteration zones of the Jaclyn and Christopher veins.

DISCUSSION

The extensive field, drillhole and regional geophysical investigations completed over the past decade, along with new petrographic, mineral, chemical and argon thermochronological data, provide important constraints on the setting and origin of the vein systems exposed at the Jaclyn

Zone gold deposit. Collectively, the data are interpreted to suggest that the mineralized systems at the Jaclyn deposit are comparable to turbidite-hosted gold deposits of the Meguma Zone in Nova Scotia (*e.g.*, Moosehead, Ovens; Sangster and Smith, 2007) and those of the prolific Bendigo-Ballarat region of southeastern Australia (*e.g.*, Bendigo, Ballarat; Bierlein *et al.*, 2000). These represent orogenic quartz-vein-hosted gold systems that are developed in volcano-sedimentary fold and thrust belts during orogenesis (Groves *et al.*, 1998, 2003).

These turbidite-hosted, orogenic vein gold deposits are typically formed in association with greenschist-facies metamorphism during crustal thickening and regional folding and thrusting. Emplacement of the veins results from the close interrelationship between progressive tectonism and the episodic upward flow of orogenic fluids. Sandeman and Copeland (2010) discussed the complex inter-relationships between the auriferous quartz veins and the Type-1 Exploits mafic dykes (Sandeman and Copeland, 2010). These dykes are commonly sausuritized and carbonatized, crosscut the veins, exhibit chilled margins and locally contain entrained xenocrysts and polycrystalline xenoliths of coarse-grained, euhedral, comb-textured quartz. They also exhibit elevated As, Sb, K₂O and CO₂ along with weakly anomalous gold (<1 to 12 ppb Au). The dykes are themselves, however, cut by quartz veins. The second set of dykes (Type-2) preserves primary clinopyroxene and plagioclase but relationships with the quartz veins were not seen. Because of their fresh character, these Type-2 dykes are inferred to postdate gold mineralization and alteration. The age of the dyke sets are not known, but Sandeman and Copeland (2010) note that one of the Type-1 dykes cuts quartz sandstones of the Badger Group (Himantian, Upper Ordovician: Williams, 1991), indicating that they must be younger than *ca.* 445 Ma (IUGS timescale, 2012). The new $^{40}\text{Ar}/^{39}\text{Ar}$ data for illite in the structural footwall of the vein indicates that some of the alteration linked to auriferous quartz veins developed at *ca.* 428 ± 2 Ma. Because the Type-1 dykes are contemporaneous with the veins, as demonstrated on the basis of cross-cutting relationships, the ages from vein-related alteration also constrain the age of these dykes to be *ca.* 428 Ma. This age is significantly older than an unpublished U/Pb zircon age of 415 ± 2 Ma for the Skull Hill Syenite, the most proximal Siluro-Devonian igneous intrusion, exposed 9 km to the west (personal communication to B. Greene by A. Halliday, 1980).

The varied orientations of the quartz veins and their textural variability (including cocks-comb and laminated veins), the contemporaneity of vein and Type-1 mafic dykes, and the abundant evidence for associated brecciation of the country rocks, attest to the recurring, episodic nature of regional deformation and accompanying crack-conduit

propagation, mafic dyke injection and the infiltration of mineralizing fluids. Sandeman *et al.* (2010) proposed that the diverse field, structural, petrographic and drillhole data could be explained by a model in which the major north-east–southwest-trending regional folds are inferred to be Salinic D₁ (*ca.* 435 Ma) structures (McNeill, 2005 *in* Copeland and Newport, 2005; Zagorevski *et al.*, 2007; van Staal *et al.*, *in press*). During progressive deformation, the folds lock up episodically as a result of fluctuation between ductile and brittle behaviour of the host rocks. Failure results in largely brittle deformation, despite substantial rheological contrast. This sporadic crack propagation and faulting is roughly axial planar to the regional D₁ folds. The cracks or faults are infiltrated by early stage hydrothermal fluid that results in the deposition of quartz veins. Continued variation in the regional stress field during progressive deformation resulted in episodic faulting along pre-existing fractures and veins, commonly accompanied by further quartz veining, alteration, gold deposition and mafic magma emplacement (fault valve behaviour; Cox, 1995).

The *ca.* 428 Ma alteration, veining and mineralization are synchronous with or postdate regional F₁ folding and aid in bracketing the timing of the Salinic event between 435 and 428 Ma (van Staal, 2007; van Staal *et al.*, *in press*). Although the age of alteration and presumably mineralization is constrained to *ca.* 428 Ma on the basis of the two identical $^{40}\text{Ar}/^{39}\text{Ar}$ cooling ages for illite developed in the immediate footwall of the quartz veins, interpretation of the date from the hanging wall of the Jaclyn Main vein is much more difficult. The presence of two distinct potassium-bearing phases means that there are 2 distinct radiogenic argon sources in the alteration assemblage. Each mineral will release its argon at differing temperatures during incremental heating, thereby resulting in a mixed age. A possible explanation for the young, *ca.* 400 Ma age for the hanging wall specimen is that the sparse illite may have grown at the same time as the illite in the footwall samples; however the adularia records a distinct, younger (Middle Devonian?) later hydrothermal event. Mixing of *ca.* 428 Ma argon with *ca.* 380 Ma argon might produce an $^{40}\text{Ar}/^{39}\text{Ar}$ gas release pattern that results in a mixed age of *ca.* 400 Ma.

Previous geochronological investigations have outlined two distinct ages of Siluro-Devonian gold deposition in the Newfoundland Appalachians (*e.g.*, Dube *et al.*, 1995; Ritcey *et al.*, 1995; McNicoll *et al.*, 2006; Kerr and van Breemen, 2007; Kerr and Selby, 2012; Minnett *et al.*, 2012). The earlier Siluro-Devonian event appears to range from *ca.* 420–405 Ma, whereas the second Middle to Late Devonian event ranges from *ca.* 385–370 Ma (Figure 6). The $^{40}\text{Ar}/^{39}\text{Ar}$ data presented herein for the Jaclyn and Christopher zones indicate that the illite alteration in the structural footwalls of two auriferous veins formed during the interval 430–426

Ma. These are the oldest ages for gold mineralization yet determined in the Newfoundland Appalachians and may suggest a previously unrecognized, early Salinic episode of orogenic gold mineralization. The adularia in the structural hanging wall of the Jaclyn Main vein may have formed during a later hydrothermal or heating event during the interval 407–393 Ma. Alternatively, the adularia may have formed at the same time as the *ca.* 428 Ma illite, but because of its lower closure temperature, was completely reset during subsequent hydrothermal fluid flow (>150°C) along the propagating vein. If this scenario is valid, then the $^{40}\text{Ar}/^{39}\text{Ar}$ data for the adularia-bearing assemblage provide a probable minimum age on the gold mineralization. Such a history of several or multiple pulses of hydrothermal fluid flow and gold mineralization is comparable to that recently presented for the orogenic Thor vein system at the Viking property in White Bay (Minett *et al.*, 2012).

ACKNOWLEDGMENTS

All of the exploration industry personnel who facilitated access to drillcore and spent much time discussing the Jaclyn vein systems are warmly thanked. In particular, I would like to acknowledge the invaluable help of Dave Copeland, Paul McNeill, Tanya Tettelaar and Jeff Morgan. Andy Kerr and Dr. Charlie Gower graciously reviewed an earlier version of this contribution. Neil Stapleton and many other Geological Survey staff are thanked for their unstinting efforts.

REFERENCES

Bierlein, F.P., Arne, D.C., McKnight, S., Lu, J., Reeves, S., Besanko, J., Marek, J. and Cooke, D. 2000: Wall-rock petrology and geochemistry in alteration haloes associated with mesothermal gold mineralization, central Victoria, Australia. *Economic Geology*, Volume 95, pages 283–312.

Copeland, D.A. and Newport, A. 2004a: Assessment report on depositing, rock and soil sampling, trenching, airborne geophysics and diamond drilling, on the Golden Promise property, central Newfoundland. Rubicon Minerals Corporation, NFLD/2902.

2004b: Supplemental 1st year assessment report on prospecting and soil sampling on the Golden Promise property, central Newfoundland, NTS 12A/16 and 02D/13. Rubicon Minerals Corporation, NFLD/2895.

2005: Supplementary 2nd year assessment report on soil sampling, depositing, geological mapping, trenching and diamond drilling on the Golden Promise property,

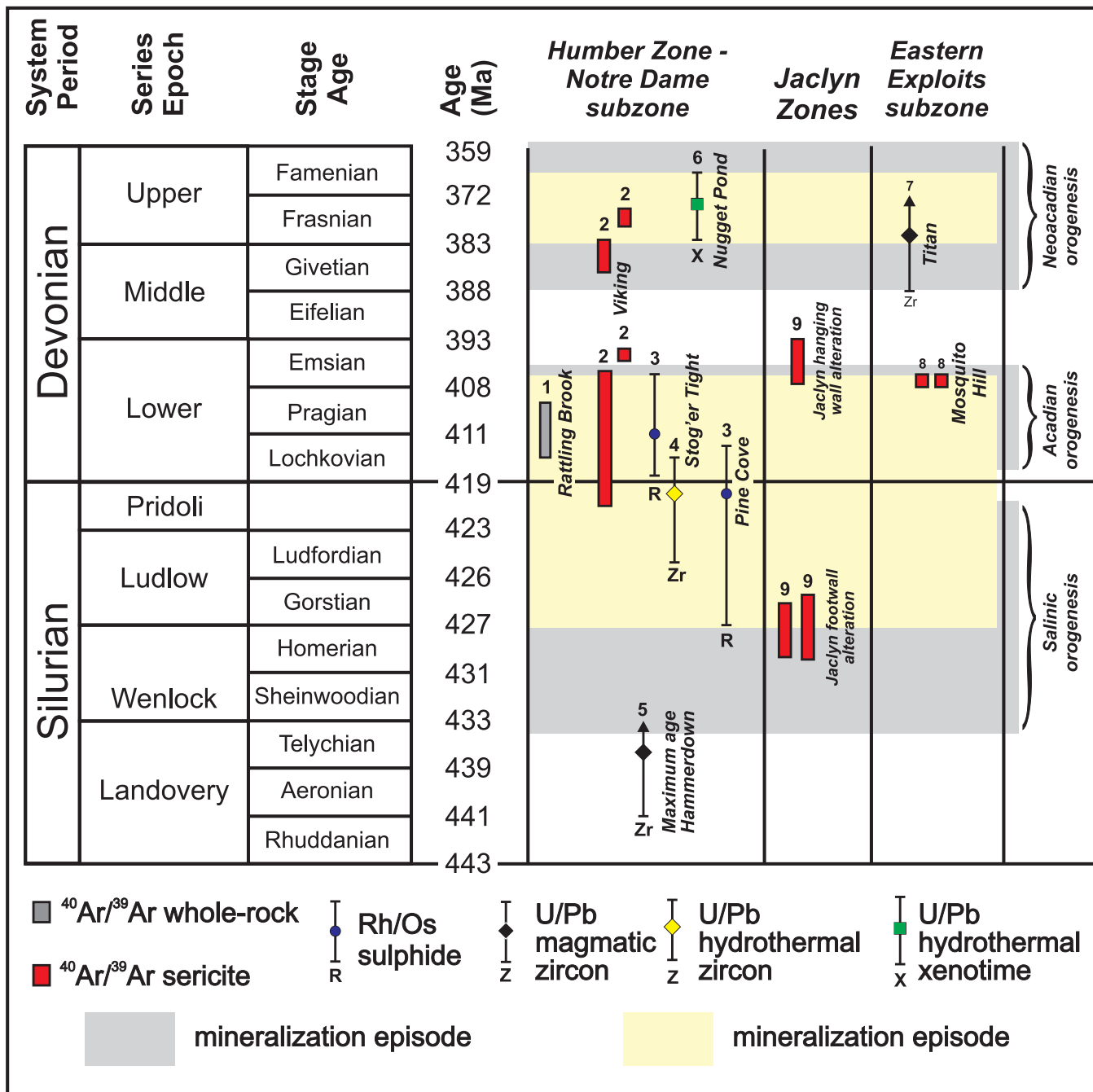


Figure 6. Summary of geochronological constraints on gold mineralizing events in the Newfoundland Appalachians (adapted after Kerr and Selby, 2012). Data sources: 1) Kerr and van Breemen (2007); 2) Minnett et al. (2012); 3) Kerr and Selby (2012); 4) Ramezani et al. (2002); 5) Ritcey et al. (1995); 6) Sangster et al. (2008); 7) McNicoll et al. (2006); 8) Sandeman et al. (2013); 9) this study.

central Newfoundland. Rubicon Minerals Corporation, NFLD/2910.

Cox, S.F.

1995: Faulting processes at high fluid pressures: an example of fault valve behavior from the Wattle Gully

Fault, Victoria, Australia. Journal of Geophysical Research, Volume 100, pages 12841-12859.

Dubé, B., Dunning, G.R., Lauzière, K. and Roddick, J.C.

1995: New insights into the Appalachian Orogen from geology and geochronology along the Cape Ray fault

zone, southwest Newfoundland. Geological Society of America Bulletin, Volume 108, pages 101-116.

Dunning, G.R., O'Brien, S.J., Colman-Sadd, S.P., Blackwood, R.F., Dickson, W.L., O'Neill, P.P. and Krogh, T.E. 1990: Silurian Orogeny in the Newfoundland Appalachians. *Journal of Geology*, Volume 98, pages 895-913.

Evans, D.T.W. and Kean, B.F. 2002: The Victoria Lake Supergroup, central Newfoundland – its definition, setting and volcanogenic massive sulphide mineralization. Newfoundland and Labrador Department of Natural Resources, Geological Survey, Open File NFLD/2790, 80 pages.

Groves, D.I., Goldfarb, R.J., Gebre-Mariam, M., Hagemann, S.G. and Robert, F. 1998: Orogenic gold deposits: a proposed classification in the context of their crustal distribution and relationship to other gold deposit types. *Ore Geology Reviews*, Volume 13, pages 7-27.

Groves, D.I., Goldfarb, R.J., Robert, F. and Hart, C.J.R. 2003: Gold deposits in metamorphic belts: overview of current understanding, outstanding problems, future research, and exploration significance. *Economic Geology*, Volume 98, pages 1-29.

Kean B.F. and Jayasinge, N.R. 1982: Geology of the Badger map area (12A/16), Newfoundland. Newfoundland Department of Mines and Energy, Mineral Development Division, Report 81-2, 37 pages.

Kerr, A., and Selby, D. 2012: The timing of epigenetic gold mineralization on the Baie Verte Peninsula, Newfoundland, Canada: new evidence from Re-Os pyrite geochronology. *Mineralium Deposita*, Volume 47, pages 325-337.

Kerr, A., and van Breemen, O. 2007: The timing of gold mineralization in White Bay, western Newfoundland: Evidence from $^{40}\text{Ar}/^{39}\text{Ar}$ studies of mafic dykes that predate and postdate mineralization. *Atlantic Geology*, Volume 43, pages 148-162.

Ludwig, K. R. 2003: ISOPLOT 3.0: A geochronological toolkit for Microsoft Excel. Geochronology Center, Special Publication, Volume 4, 71 pages.

McDougall, I. and Harrison, T.M. 1988: Geochronology and thermochronology by the $^{40}\text{Ar}/^{39}\text{Ar}$ method: Oxford Monographs on Geology and Geophysics #9, Oxford, United Kingdom, Oxford University Press, 212 pages.

McNicol, V., Squires, G.C., Wardle, R.J., Dunning, G.R. and O'Brien, B.H. 2006: U-Pb geochronological evidence for Devonian deformation and gold mineralization in the eastern Dunnage Zone, Newfoundland. *In Current Research. Newfoundland and Labrador Department of Natural Resources, Geological Survey, Report 06-1*, pages 43-60.

Minnett, M., Sandeman, H.S. and Wilton, D.H.C. 2012: Geochemistry of the host rocks and timing of gold-electrum mineralization at the Viking property, Newfoundland. *In Current Research. Newfoundland and Labrador Department of Natural Resources, Geological Survey, Report 12-1*, pages 61-84.

Mullen, D. 2003: First year assessment report on trenching and diamond drilling exploration for licences 8859M and 8868M on claims in the Exploits River area, southwest of Badger, central Newfoundland. Newfoundland and Labrador Geological Survey, Assessment File 12A/16/1047, 192 pages.

Newport, A.M. 2003: A comparison of auriferous boulders to a potential bedrock source, Golden Promise Prospect, Badger, Newfoundland (N.T.S. 12A/16). Unpublished B.Sc. Thesis, Memorial University of Newfoundland, St. John's, 125 pages.

Pilgrim, L.R. and Giroux, G.H. 2008: Form 43-101F1 technical report for the Golden Promise, south Golden Promise and Victoria Lake properties Badger, Grand Falls, Buchans and Victoria Lake areas (NTS 12A/06, 09, 10, 15, 16 and 02D/13), Newfoundland and Labrador. Crosshair Exploration and Mining Corporation SEDAR filing.

Ramezani, J., Dunning, G.R. and Wilson, M.R. 2002: Geologic setting, geochemistry of alteration, and U-Pb age of hydrothermal zircon from the Silurian Stog 'er Tight gold prospect, Newfoundland Appalachians, Canada. *Exploration and Mining Geology*, Volume 9, pages 171-188.

Reynolds, P.H. 1992: Low temperature thermochronology by the $^{40}\text{Ar}/^{39}\text{Ar}$ method. *In Low Temperature Thermochronology. Edited by M. Zentilli and P.H. Reynolds. Mineralogical Association of Canada*, pages 3-19.

Ritcey, D.H., Wilson, M.R. and Dunning, G.R.
1995: Gold mineralization in the Paleozoic Appalachian Orogen: Constraints from geologic, U-Pb and stable isotope studies of the Hammerdown prospect, Newfoundland. *Economic Geology*, Volume 90, pages 1955-1965.

Rogers, N. and van Staal, C.
2002: Toward a Victoria Lake Supergroup: a provisional stratigraphic revision of the Red Indian to Victoria lakes area, central Newfoundland. *In Current Research. Newfoundland Department of Natural Resources, Geological Survey, Report 02-1*, pages 185-195.

Rogers, N., van Staal, C. and McNicoll, V.J.
2005: Geology, Badger, Newfoundland and Labrador: Geological Survey of Canada, Open File 4546, scale 1:50,000.

Sandeman, H. and Copeland, D.
2010: Preliminary lithogeochemistry for Exploits dykes from the Badger map area, Exploits Subzone, central Newfoundland. *In Current Research. Newfoundland Department of Natural Resources, Geological Survey, Report 10-1*, pages 65-76.

Sandeman, H., Rafuse, H. and Copeland, D.
2010: The setting of orogenic, auriferous quartz veins at the Golden Promise prospect, central Newfoundland and observations on veining and wall-rock alteration. *In Current Research. Newfoundland and Labrador Department of Natural Resources, Geological Survey, Report 10-1*, pages 77-92.

Sandeman, H.A., Wilton, D.H.C., Conliffe, J., Froude, T. and O'Driscoll, J.M.
2013: Geological setting, geochronological constraints and the nature of mineralization at the Mosquito Hill (Huxter Lane) gold deposit, central Newfoundland. *In Current Research. Newfoundland Department of Natural Resources, Geological Survey, Report 13-1*, pages 167-188.

Sangster, A.L., Douma, S.L. and Lavigne, L.
2008: Base metal and gold deposits of the Betts Cove Complex, Baie Verte Peninsula, Newfoundland. *In Mineral Deposits of Canada: A Synthesis of Major Deposit Types, District Metallogeny, the Evolution of Geological Provinces and Exploration Methods. Edited by W.D. Goodfellow. Geological Survey of Canada, Mineral Deposits Division, Special Volume 5*, pages 703-723.

Sangster, A.L. and Smith, P.K.
2007: Metallogenetic summary of the Meguma gold deposits, Nova Scotia. *In Mineral Deposits of Canada: A Synthesis of Major Deposit Types, District Metallogeny, the Evolution of Geological Provinces, and Exploration Methods. Edited by W.D. Goodfellow. Geological Association of Canada, Mineral Deposits Division, Special Publication 5*, pages 723-732.

Singer, B.S. and Pringle, M.S.
1996: Age and duration of the Matuyama-Brunhes geomagnetic polarity reversal from $^{40}\text{Ar}/^{39}\text{Ar}$ incremental heating analyses of lavas. *Earth and Planetary Science Letters*, Volume 139, pages 47-61.

Snee, L.W., Sutter, J.F. and Kelly, W.C.
1988: Thermochronology of economic mineral deposits; dating the stages of mineralization at Panasqueira, Portugal, by highprecision 40 / 39 Ar age spectrum techniques on muscovite. *Economic Geology*, Volume 83, pages 335-354.

Tarnocai, C.
2004: Geological interpretation and target selection at Golden Promise, Newfoundland. Placer Dome confidential report.

van Staal, C.R.
2007: Pre-Carboniferous tectonic evolution and metallogeny of the Canadian Appalachians. *In Mineral Deposits of Canada: A Synthesis of Major Deposit Types, District Metallogeny, the Evolution of Geological Provinces, and Exploration Methods. Edited by W.D. Goodfellow. Geological Association of Canada, Mineral Deposits Division, Special Publication 5*, pages 793-818.

van Staal, C.R., Zagorevski, A., McNicoll, V.J. and Rogers, N.
In press: The time-transgressive Salinic and Acadian orogenesis, magmatism and Old Red sandstone sedimentation in Newfoundland. *Geoscience Canada*.

Waldrone, J.W.F., McNicoll, V.J. and van Staal, C.R.
2012: Laurentia-derived detritus in the Badger Group of central Newfoundland: Deposition during closing of the Iapetus Ocean. *Canadian Journal of Earth Sciences*, Volume 49, pages 207-221.

Williams, H.
1995: Chapter 4 – Middle Paleozoic rocks. *In Geology of the Appalachian-Caledonide Orogen in Canada and*

Greenland. Edited by H. Williams. Geological Survey of Canada, Geology of Canada Series No. 6, pages 315-446.

Williams, H., Colman-Sadd, S.P. and Swinden, H.S. 1988: Tectonic stratigraphic subdivisions of central Newfoundland. In Current Research, Part B. Geological Survey of Canada, Paper 88-1B, pages 91-98.

Williams, S.H. 1991: Stratigraphy and graptolites of the Upper Ordovician Point Leamington Formation, central Newfoundland. Canadian Journal of Earth Sciences, Volume 28, pages 581-600.

Williams, S.H. and O'Brien, B.H. 1991: Silurian graptolites from the Bay of Exploits, north-central Newfoundland and their geological significance. Canadian Journal of Earth Sciences, Volume 28, pages 1534-1540.

Zagorevski, A., van Staal, C.R. and McNicoll, V.J. 2007: Distinct Taconic, Salinic, and Acadian deformation along Iapetus suture zone, Newfoundland Appalachians. Canadian Journal of Earth Sciences, Volume 44, pages 1567-1585.

